Mannose receptor regulates myoblast motility and muscle growth

Katie M. Jansen[1,2] and Grace K. Pavlath[1]

[1]Department of Pharmacology and [2]Program in Biochemistry, Cell, and Developmental Biology, Emory University, Atlanta, GA 30322

Myoblast fusion is critical for the formation, growth, and maintenance of skeletal muscle. The initial formation of nascent myotubes requires myoblast–myoblast fusion, but further growth involves myoblast–myotube fusion. We demonstrate that the mannose receptor (MR), a type I transmembrane protein, is required for myoblast–myotube fusion. Mannose receptor (MR)–null myotubes were small in size and contained a decreased myonuclear number both in vitro and in vivo. We hypothesized that this defect may arise from a possible role of MR in cell migration. Time-lapse microscopy revealed that MR-null myoblasts migrated with decreased velocity during myotube growth and were unable to migrate in a directed manner up a chemoattractant gradient. Furthermore, collagen uptake was impaired in MR-null myoblasts, suggesting a role in extracellular matrix remodeling during cell motility. These data identify a novel function for MR during skeletal muscle growth and suggest that myoblast motility may be a key aspect of regulating myotube growth.

Introduction

Skeletal muscle is composed of multinucleated myofibers that form through the process of myogenesis. During myogenesis, myoblasts must exit the cell cycle and subsequently undergo differentiation and cell–cell fusion to form myofibers in vivo or myotubes in vitro. Myoblast fusion follows an ordered set of cellular events, including cell migration, adhesion, and membrane fusion (Knudsen and Horwitz, 1977). Myoblast fusion is important not only for skeletal muscle formation during development but also for the postnatal regeneration and growth of skeletal muscle.

Mammalian myoblast fusion occurs in two phases (Horsley and Pavlath, 2004). Initially, myoblasts fuse with one another to form small, nascent myotubes. Additional myoblasts subsequently fuse with nascent myotubes, leading to the formation of large, mature myotubes. Although several molecules regulating the first phase of fusion have been identified, few molecules specifically regulating the fusion of myoblasts with nascent myotubes are known (Horsley and Pavlath, 2004). Molecules implicated to function during the second stage of fusion include secreted proteins and membrane bound proteins, as well as transcription factors. Follistatin (Iezzi et al., 2004), prostaglandin F2α (Horsley and Pavlath, 2003), and interleukin-4 (IL-4; Horsley et al., 2003) are secreted by muscle cells and enhance the growth of nascent myotubes. Prostaglandin F2α–mediated growth is dependent on the transcription factor NFATC2 (nuclear factor of activated T cells, cytoplasmic, calcineurin-dependent 2; Horsley et al., 2001), and NFATC2 regulates expression of IL-4 (Horsley et al., 2003). IL-4 is secreted by a subset of nascent myotubes and acts on unfused cells, leading to their recruitment and fusion with nascent myotubes. In addition, an unknown secreted factor is responsible for mammalian target of rapamycin's actions in regulating myoblast–myotube fusion (Park and Chen, 2005). Membrane bound proteins are also important, as myoferlin, a protein localized to the intracellular region of the plasma membrane, is required for the formation of large myotubes (Doherty et al., 2005). Finally, the lectin wheat germ agglutinin inhibits the second stage of fusion in vitro (Muroya et al., 1994), suggesting that carbohydrate binding proteins likely play an important role during this phase of fusion. The mechanisms by which these molecules regulate the second stage of myoblast fusion have not been identified.

The mannose receptor (MR) is a 175-kD type 1 transmembrane protein that binds a variety of soluble and cell surface glycoproteins (Otter et al., 1991; Pontow et al., 1992; Martinez-Pomares and Gordon, 1999; Linehan et al., 2001; Martinez-Pomares et al., 2001) and is one of four members of the MR family of proteins (East and Isacke, 2002). The extracellular region of MR consists of three types of domains: an

Correspondence to Grace K. Pavlath: gpavlat@emory.edu

Abbreviations used in this paper: DM, differentiation media; eMyHC, embryonic myosin heavy chain; GM, growth media; H&E, hematoxylin and eosin; IL-4, interleukin-4; MR, mannose receptor; RV, retrovirus; TA, tibialis anterior; WT, wild-type; XSA, cross-sectional area.

The online version of this article contains supplemental material.

The Journal of Cell Biology, Vol. 174, No. 3, July 31, 2006 403–413
http://www.jcb.org/cgi/doi/10.1083/jcb.200601102

N-terminal cysteine-rich domain that confers MR's ability to bind sulfated sugars (Fiete et al., 1998), a region of fibronectin type II repeats responsible for binding collagen (East and Isacke, 2002; Martinez-Pomares et al., 2006; Napper et al., 2006), and eight carbohydrate recognition domains, providing terminal mannose, fucose, N-acetylglucosamine, and glucose binding ability in a calcium-dependent manner (Taylor et al., 1992). MR is an endocytic receptor and contains a 45-amino-acid cytoplasmic region thought to be responsible for receptor internalization (Kruskal et al., 1992). MR is expressed in a variety of tissues and has been proposed to function in serum glycoprotein clearance, antigen transport and presentation, and immune cell recognition of foreign microbes (Ezekowitz et al., 1991; Schlesinger, 1993; Martinez-Pomares and Gordon, 1999; Lee et al., 2002). Several lines of indirect evidence have suggested that terminal mannose residues or MR may function in cell fusion. MR expression increases in hematopoietic precursors undergoing differentiation and peaks during cell fusion to form osteoclasts or multinucleated giant cells (Morishima et al., 2003). High mannose mannan, which binds MR with high affinity, inhibits the fusion of macrophages during multinucleated giant cell formation in vitro (McNally et al., 1996). In addition, the mannose binding compound pradimicin and an inhibitor of glucosidase I, an enzyme required for high mannose oligosaccharide expression, prevent the fusion of hematopoietic precursor cells during osteoclast formation (Kurachi et al., 1994; Morishima et al., 2003). MR also functions in cell–cell adhesion, as antibodies that recognize MR inhibit lymphocyte adhesion to endothelial cells in vitro (Irjala et al., 2003).

IL-4 signaling regulates MR expression in several cell types (Stein et al., 1992; Sallusto et al., 1995; Linehan et al., 2003; Martinez-Pomares et al., 2003; Zimmer et al., 2003). Because IL-4 is a known regulator of myoblast fusion and because carbohydrate binding proteins have been implicated in fusion, we hypothesized that MR may have an important function during myogenesis. Here, we demonstrate that MR is required for myoblast fusion with nascent myotubes in vitro and for proper skeletal muscle growth in vivo. We also provide the first evidence that MR plays an important role in cell motility, as $MR^{-/-}$ cells have impaired migratory speed during myoblast fusion in vitro. In addition, we show that the collagen uptake is impaired in $MR^{-/-}$ cells and that MR is required for directed cell migration during myotube growth. Importantly, these data identify a novel function for MR during skeletal muscle growth and have a broad implication for MR regulation of cell motility.

Results

MR is expressed during myoblast fusion

To determine whether MR is expressed in muscle cells during fusion, myoblasts were induced to differentiate by switching to differentiation media (DM) for 0, 24, or 48 h. After 24 h in DM, myoblasts fused to form small, nascent myotubes, and after 48 h, large myotubes had formed (Fig. 1 A). RT-PCR analyses revealed that MR mRNA levels increased after the onset of myoblast fusion and remained elevated at 48 h (Fig. 1 A). RT-PCR analyses of myogenin expression, a marker of myogenic differentiation (Wright et al., 1989), demonstrated that the increase in MR expression was concurrent with the onset of differentiation. Immunostaining of muscle cells after 24 h in DM with an antibody against the intracellular portion of MR (Burudi and Regnier-Vigouroux, 2001) revealed that MR protein was present in both mononucleated cells and nascent myotubes (Fig. 1 B). No immunostaining was present in $MR^{-/-}$ muscle cells (Lee et al., 2002), indicating the specificity of the antibody.

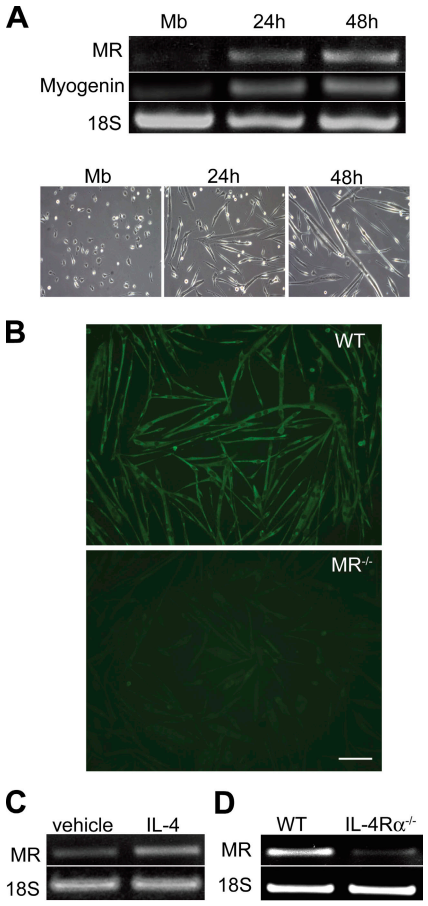

Figure 1. **MR is expressed in muscle cells during myoblast fusion.** (A) Primary myoblasts (Mb) were induced to differentiate for 24 or 48 h. MR mRNA was analyzed by RT-PCR. Myogenin mRNA was assessed as a marker of myogenic differentiation. Phase-contrast images of muscle cells are shown to illustrate fusion progress at each time point. MR, 390 bp; Myogenin, 266 bp; 18S, 488 bp. (B) Representative images of muscle cells after 24 h of differentiation immunostained with an antibody against MR. Bar, 50 μm. (C) Primary myoblasts were differentiated for 24 h and subsequently treated with vehicle or 10 ng/ml IL-4 for 24 h. MR mRNA was analyzed by RT-PCR. (D) MR mRNA expression in WT or IL-4 receptor α-null ($IL\text{-}4R\alpha^{-/-}$) myotubes after 48 h in DM was examined by RT-PCR. MR, 390 bp; 18S, 488 bp. Representative ethidium bromide staining of agarose gels is shown with 18S ribosomal RNA as an internal control for all RT-PCR analyses. All data are indicative of results from three independent cell isolates.

IL-4 signaling regulates MR expression in several cell types (Stein et al., 1992; Sallusto et al., 1995; Linehan et al., 2003; Martinez-Pomares et al., 2003; Zimmer et al., 2003). IL-4–mediated regulation of MR expression in muscle cells was assessed in two experiments. First, nascent myotubes were treated with recombinant IL-4 for 24 h. RT-PCR analyses indicated that MR mRNA levels increased in myotubes treated with

IL-4 (Fig. 1 C). Conversely, MR mRNA expression was reduced in myotubes deficient of the IL-4 receptor (Fig. 1 D, IL-4Rα$^{-/-}$). Together, these data suggest that IL-4 signaling regulates MR expression in fusing myoblasts.

MR is required for the second stage of myoblast fusion

To test the hypothesis that MR is involved in myoblast fusion, we examined the ability of myoblasts derived from wild-type (WT) or MR$^{-/-}$ mice (Lee et al., 2002) to form myotubes in vitro. After 20 or 48 h in DM, cells were immunostained with an antibody against embryonic myosin heavy chain (eMyHC; Fig. 2 A), marking the cytoplasm of differentiated muscle cells and clearly defining the nuclei of myotubes. After 20 h in DM, MR$^{-/-}$ myoblasts fused to form small myotubes indistinguishable from WT myotubes. However, by 48 h in DM, WT myoblasts formed large myotubes, whereas MR$^{-/-}$ myotubes remained small. The impaired growth of MR$^{-/-}$ myotubes could arise from several factors, including defects in proliferation, differentiation, or fusion. To assess the requirement of MR in myoblast proliferation, WT and MR$^{-/-}$ myoblasts were pulsed for 1 h with BrdU. The percentage of BrdU^{+} cells was similar in WT and MR$^{-/-}$ cells, indicating that MR is not required for myoblast proliferation (Fig. S1 A, available at http://www.jcb.org/cgi/content/full/jcb.200601102/DC1). To determine whether MR$^{-/-}$ myoblasts underwent impaired or delayed differentiation, we assessed expression of two markers of myogenic differentiation. Immunoblots were performed to examine myogenin expression at 16 h in DM, before myoblast fusion. WT and MR$^{-/-}$ cells expressed similar levels of myogenin (Fig. 2 B), demonstrating that early stages of myogenic differentiation were not disrupted in MR$^{-/-}$ cells. The percentage of nuclei found in eMyHC^{+} cells after 48 h in DM was not decreased in MR$^{-/-}$ cells (Fig. 2 C), indicating that MR is not required for the later stages of myogenic differentiation. In addition, similar numbers of nuclei were present in WT and MR$^{-/-}$ cultures after 48 h in DM (Fig. S1 B), indicating that cell survival is not disrupted in MR$^{-/-}$ cells during differentiation and fusion.

To determine whether MR$^{-/-}$ myoblasts form small myotubes as a result of defects in myoblast fusion, two types of fusion analyses were performed. The fusion indices were calculated as the percentage of nuclei located in myotubes (≥2 nuclei) after 48 h in DM and were similar for WT and MR$^{-/-}$ cells (Fig. 2 D), indicating that MR$^{-/-}$ cells do not have a general defect in myoblast fusion. The number of nuclei contained within WT and MR$^{-/-}$ myotubes was next quantified (Fig. 2 E). After 20 h in DM, MR$^{-/-}$ myotubes contained the same mean number of nuclei as WT myotubes, indicating that the first stage of myoblast fusion is not disrupted in MR$^{-/-}$ cells. After 48 h in DM, however, MR$^{-/-}$ myotubes contained significantly fewer nuclei than WT myotubes. Importantly, MR$^{-/-}$ cells do not form small myotubes as a result of delayed myoblast fusion, as the number of nuclei in MR$^{-/-}$ myotubes remained low, even after 72 h in DM. These data suggest that MR is required for the second stage of myoblast fusion, during which myoblasts fuse with nascent myotubes (Horsley and Pavlath, 2004).

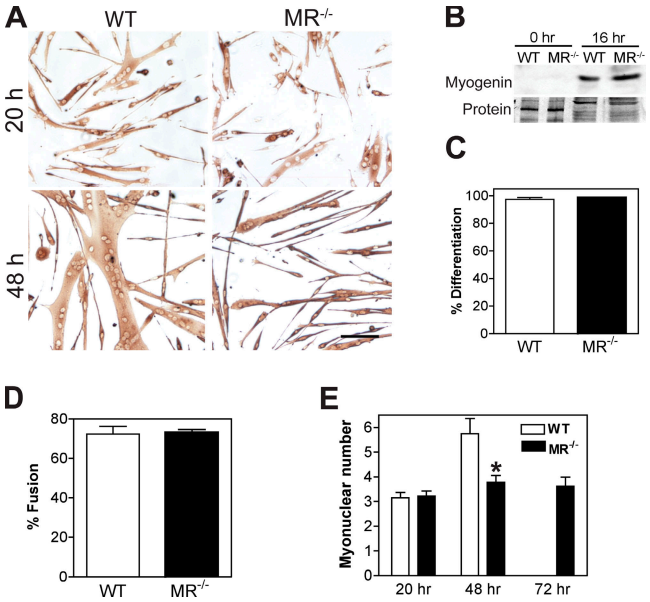

Figure 2. **MR is required for the second phase of myoblast fusion in vitro.** (A) WT and MR$^{-/-}$ myoblasts were induced to differentiate in DM for 20 or 48 h, followed by immunostaining for eMyHC. Bar, 60 μm. (B) Myogenin levels in WT and MR$^{-/-}$ cells were assessed by immunoblot analysis of cell lysates collected after 0 or 16 h in DM. Coomassie staining of the membrane is shown to demonstrate equal loading. (C) The percentage of nuclei within eMyHC^{+} WT and MR$^{-/-}$ cells was calculated after 48 h in DM. (D) The percentage of nuclei within WT and MR$^{-/-}$ myotubes (≥2 nuclei) was calculated after 48 h in DM. (E) The number of nuclei in individual WT and MR$^{-/-}$ myotubes (≥2 nuclei) was analyzed after 20, 48, or 72 h in DM. The mean number of myonuclei is decreased in MR$^{-/-}$ myotubes compared with WT at 48 h. Data are mean ± SEM for three independent cell isolates. *, $P < 0.05$.

MR is required for normal skeletal muscle growth

Our in vitro data establish a role for MR during myoblast fusion. To determine whether MR plays a functional role in skeletal muscle in vivo, we examined myofiber size in WT and MR$^{-/-}$ muscles. The tibialis anterior (TA) muscles were collected from adult WT and MR$^{-/-}$ mice, and sections were stained with hematoxylin and eosin (H&E; Fig. 3 A). As confirmed by cross-sectional area (XSA) analyses (Fig. 3 B), MR$^{-/-}$ myofibers were significantly smaller than WT myofibers. In addition, WT muscles contained a higher percentage of large myofibers, whereas MR$^{-/-}$ muscles contained a higher percentage of small myofibers (Fig. 3 C). Myonuclear number analyses were performed (Horsley et al., 2001; Mitchell and Pavlath, 2001) on TA muscle sections to determine whether MR$^{-/-}$ myofibers contain fewer myonuclei than WT myofibers, as was observed in myotubes in vitro. MR$^{-/-}$ myofibers contained significantly fewer myonuclei than WT myofibers (Fig. 3 D), suggesting that the reduced XSA of MR$^{-/-}$ myofibers is at least partially due to a decrease in myonuclear number (Allen et al., 1999). XSA analyses were also performed on WT and MR$^{-/-}$ soleus muscles to ensure that the reduced myofiber size was not specific to the TA. Mean myofiber XSA was also significantly reduced in MR$^{-/-}$ soleus muscles (Fig. 3 E). However, the number of myofibers in MR$^{-/-}$ soleus muscles was not significantly different than WT (Fig. 3 F).

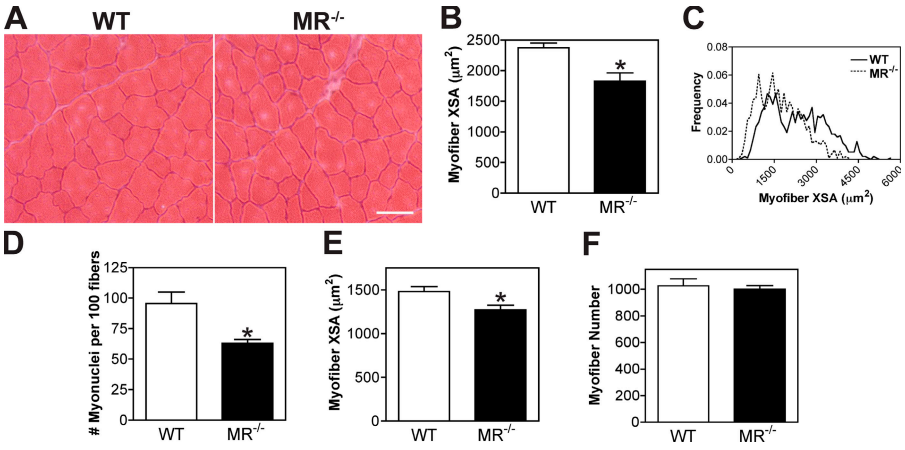

Figure 3. **Myofiber XSA and myonuclear number are decreased in MR$^{-/-}$ muscle.** (A) Representative sections of WT and MR$^{-/-}$ TA muscles stained with H&E. Bar, 60 μm. (B) Mean myofiber XSA was calculated for WT and MR$^{-/-}$ TA muscles. The mean XSA of MR$^{-/-}$ TA myofibers is reduced by 23% compared with WT. Data are mean ± SEM. n = 5–6 per genotype. *, $P < 0.01$. (C) Frequency histogram showing the distribution of myofiber XSA in WT (n = 943 myofibers) and MR$^{-/-}$ (n = 1,057 myofibers) TA muscles. (D) The mean myonuclear number of MR$^{-/-}$ TA myofibers is reduced by ∼34% compared with WT. Data are mean ± SEM. n = 5 for each genotype. *, $P < 0.05$. (E) Mean myofiber XSA was calculated for WT and MR$^{-/-}$ soleus muscles. The mean XSA of MR$^{-/-}$ soleus myofibers is reduced by 14% compared with WT. Data are mean ± SEM. n = 5 for each genotype. *, $P < 0.05$. (F) No difference is observed in the mean number of myofibers per soleus muscle of WT and MR$^{-/-}$ mice. Data are mean ± SEM. n = 5 for each genotype.

Together, these data suggest that MR is required for developmental muscle growth or maintenance in vivo.

To examine MR function specifically in skeletal muscle growth, we analyzed myofiber growth in WT and MR$^{-/-}$ mice after muscle injury. $BaCl_2$ was injected into the TA muscles of adult mice to induce injury (Caldwell et al., 1990; McArdle et al., 1994). After 5, 7, and 14 d of regeneration, muscles were collected, sectioned, and stained with H&E (Fig. 4 A). XSA analyses revealed that WT and MR$^{-/-}$ myofibers were similar in size at early stages of muscle repair (5 d after injury), but MR$^{-/-}$ myofibers were impaired in growth at later stages (7–14 d after injury; Fig. 4 B). By 14 d of regeneration, both WT and MR$^{-/-}$ myofibers had returned to their respective uninjured size. These data provide further evidence for the requirement of MR function during the later stages of muscle growth.

MR acts in mononucleated cells during fusion with nascent myotubes

MR may function in mononucleated cells and/or nascent myotubes during the second stage of myoblast fusion. If MR functions in mononucleated cells, MR$^{-/-}$ mononucleated cells should not be recruited to fuse with WT nascent myotubes. To test this hypothesis, WT nascent myotubes were cocultured with MR$^{-/-}$ mononucleated cells in DM for 24 h (Fig. 5 A). Before coculture, each cell population was stained with a fluorescent dye (Horsley et al., 2003). After coculture, myotubes were analyzed for the presence of both fluorescent dyes. Coculture of WT nascent myotubes with WT mononucleated cells resulted in 77% of myotubes containing both fluorescent dyes (Fig. 5 B). In contrast, coculture of WT nascent myotubes with MR$^{-/-}$ mononucleated cells resulted in only 37% of myotubes containing both fluorescent dyes, indicating that MR$^{-/-}$ mononucleated cells are impaired in their ability to fuse with nascent myotubes. To determine whether MR functions in nascent myotubes, MR$^{-/-}$ nascent myotubes were cocultured with WT mononucleated cells. After coculture, ∼63% of myotubes contained both fluorescent dyes. These results are not statistically different from WT/WT coculture, suggesting that MR function is not also required in nascent myotubes. To confirm the requirement of MR function during the second stage of fusion, we cocultured MR$^{-/-}$ nascent myotubes with MR$^{-/-}$ mononucleated cells. As expected, MR deficiency led to a significant reduction in myoblast fusion with nascent myotubes, as only 32% of myotubes contained both fluorescent dyes. Together, these

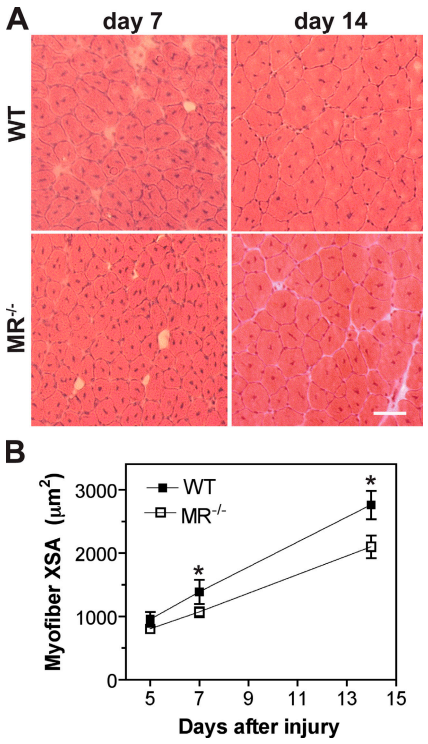

Figure 4. **MR is required for normal muscle regeneration after injury.** (A) At days 7 and 14 after $BaCl_2$ injury, WT and MR$^{-/-}$ TA sections were stained with H&E. Representative sections are shown. Bar, 50 μm. (B) The XSA of regenerating myofibers was analyzed 5, 7, or 14 d after injury. The mean XSA of MR$^{-/-}$ myofibers 7 and 14 d after injury is significantly reduced compared with WT. Data are mean ± SEM. n = 5–6 per time point for each genotype. *, $P < 0.001$.

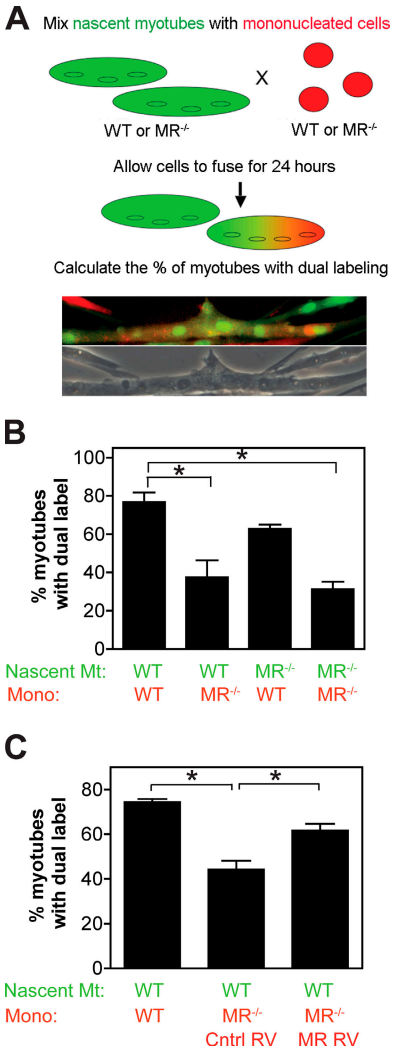

Figure 5. **MR is required in mononucleated cells for normal fusion with nascent myotubes.** (A) WT or $MR^{-/-}$ nascent myotubes were labeled with a green fluorescent dye and mixed with WT or $MR^{-/-}$ mononucleated cells labeled with a red fluorescent dye. After 24 h in DM, myotubes were fixed and analyzed for dual labeling. A representative myotube with dual labels is shown. (B) The percentage of myotubes with dual labels was calculated for each mixing experiment as indicated. The percentage of myotubes with dual labeling was significantly reduced when WT nascent myotubes were mixed with $MR^{-/-}$ mononucleated cells compared with WT mononucleated cells. (C) Retroviral-mediated expression of MR (MR RV) in $MR^{-/-}$ mononucleated cells rescues the defect in fusion with WT nascent myotubes. Data are mean ± SEM for three independent cell isolates. *, $P < 0.05$.

data suggest that mononucleated cells are the primary site of MR function during their fusion with nascent myotubes.

To determine whether the impaired ability of $MR^{-/-}$ mononucleated cells to fuse with nascent myotubes results specifically from a loss of MR function, MR expression was restored in $MR^{-/-}$ muscle cells via retroviral infection (Martinez-Pomares et al., 2003). Coculture of $MR^{-/-}$ mononucleated cells infected with a MR retrovirus (RV) significantly increased the ability of these cells to fuse with WT nascent myotubes compared with $MR^{-/-}$ mononucleated cells infected with a control RV (Fig. 5 C). Together, these results indicate that MR is required for proper fusion of mononucleated cells with nascent myotubes.

MR influences myogenic cell motility

We hypothesized that MR may regulate the second stage of myoblast fusion by influencing cell–cell adhesion or cell motility. Cell–cell adhesion assays indicated that $MR^{-/-}$ muscle cells were not defective in their ability to adhere with one another in suspension (unpublished data). To determine whether MR regulates muscle cell motility, we performed time-lapse microscopy of WT and $MR^{-/-}$ cells undergoing fusion in vitro. After 0 or 24 h in DM, cell movements were recorded every 5 min for 3 h. The paths of individual mononucleated cells were tracked, revealing that WT cells migrated farther than $MR^{-/-}$ cells (Fig. 6 A). Additionally, the mean velocity of $MR^{-/-}$ cells was reduced 23% compared with WT cells after 24 h in DM (Fig. 6 B), with a greater percentage of WT cells migrating at high velocities compared with $MR^{-/-}$ cells (Fig. 6 C). Importantly, retroviral-mediated MR expression in $MR^{-/-}$ cells significantly increased the mean cell velocity compared with $MR^{-/-}$ cells infected with a control RV (Fig. 6 D). To ensure that retroviral infection of myoblasts does not alter cell motility, we assessed the migration of control or RV-infected WT cells after 24 h in DM. The motility of RV-infected cells was not disrupted (Fig. S2, available at http://www.jcb.org/cgi/content/full/jcb.200601102/DC1), suggesting that the differences in cell velocity shown in Fig. 6 (B and D) are due to variability between sets of cell isolates and not the infection process. The mean velocity of $MR^{-/-}$ cells before the first stage of myoblast fusion (0–3 h in DM) was not significantly different from WT (Fig. 6 B). These data demonstrate the requirement of MR for efficient motility of myogenic cells during their fusion with nascent myotubes.

MR is required for directed migration and collagen uptake

The decreased velocity of $MR^{-/-}$ cells during myoblast fusion may result from a defect in random or directed cell migration. To distinguish between these possibilities, we tested the ability of $MR^{-/-}$ cells to respond to a chemotactic gradient. If MR is required for a directional response of muscle cells to a chemoattractant during myotube growth, we reasoned that such a factor should be present in conditioned media from nascent myotube cultures. Dunn chemotaxis chambers were used to establish a gradient of conditioned media, and the migratory response of muscle cells was observed over 3 h by time-lapse microscopy. The paths of individual cells were tracked, and the final location of each cell in relation to its origin was determined. Directional data were summarized in circular histograms, and statistical tests revealed that WT but not $MR^{-/-}$ cells migrated up a gradient of conditioned media (Fig. 7 A). Conditioned media also contains chemokinetic properties not dependent on MR, as the velocity of both WT and $MR^{-/-}$ cells increased 1.2–1.5-fold in the presence of a conditioned media gradient (Fig. 7 B). The mean velocity of $MR^{-/-}$ cells was significantly lower than WT cells in the presence of control or conditioned media, confirming that MR is required for efficient motility of muscle cells in addition to functioning in directed migration.

The MR family member Endo180 plays a role in both directed and random cell migration (East et al., 2003; Sturge

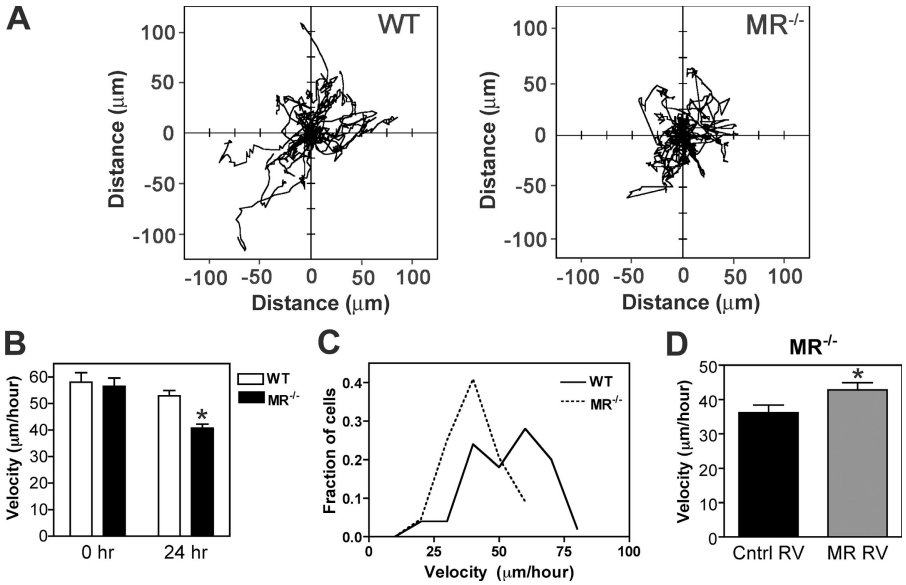

Figure 6. **MR is required for efficient muscle cell motility.** (A) After 24 h in DM, time-lapse photographs of WT and $MR^{-/-}$ cells were taken every 5 min for 3 h. The migratory paths of individual mononucleated cells are shown. Paths of 10 cells from each of three independent cell isolates for each genotype were pooled for a total of 30 cell paths. (B) The mean velocities of WT and $MR^{-/-}$ cells were pooled from three independent cell isolates at 0–3 h or 24–27 h in DM. The mean velocity of $MR^{-/-}$ cells is reduced by 23% compared with WT from 24–27 h in DM. Data are mean ± SEM. $n = 45$–50 cells. *, $P < 0.0001$. (C) Frequency histogram showing the distribution of velocities for WT and $MR^{-/-}$ cells. (D) $MR^{-/-}$ cells were infected with control or MR RV. After 24 h in DM, time-lapse photographs were taken every 5 min for 3 h. The mean velocities were pooled from three independent cell isolates. RV-mediated MR expression significantly increases the velocity of $MR^{-/-}$ cells. Data are mean ± SEM. *, $P < 0.05$.

et al., 2003). Endo180 is thought to facilitate cell motility via clearance of collagen, a component of the ECM. Degradation of the ECM is an important step in facilitating cell migration during tissue development, regeneration, and homeostasis (Murphy and Gavrilovic, 1999). Recently, MR was shown to bind collagen, most likely through its fibronectin type II repeats (Martinez-Pomares et al., 2006; Napper et al., 2006). To determine whether MR facilitates collagen clearance in muscle cells, we performed uptake assays with ^{125}I-labeled type IV collagen. Differentiating $MR^{-/-}$ muscle cells internalized significantly less collagen than WT cells (Fig. 8). Together, these results demonstrate that MR functions in directed migration of muscle cells and suggest that MR facilitates cell motility by internalizing collagen during myotube growth.

Discussion

Skeletal muscle formation, growth, and regeneration rely on the fusion of mononucleated myoblasts with one another and with existing myofibers. Myoblast fusion is dependent on a series of cellular events, including myoblast differentiation, migration, adhesion, and membrane breakdown. Disruption of any of these processes may inhibit myoblast fusion. The molecular pathways regulating myoblast fusion in mammals are largely unclear. Here, we show that MR, a type I transmembrane protein, is required for the normal fusion of myoblasts with nascent myotubes. MR plays an important role in muscle cell motility, as $MR^{-/-}$ myoblasts migrate at reduced velocity during myotube growth and directed migration up a chemoattractant gradient is ablated. In addition, collagen uptake is impaired, suggesting a role for MR in ECM remodeling during cell migration.

Myoblast fusion in mammals occurs in two phases (Horsley and Pavlath, 2004). Initially, myoblasts fuse with one another to form small, nascent myotubes. Subsequently, myonuclear accretion occurs through the fusion of additional myoblasts with nascent myotubes. Our data indicate that MR is required during the second stage of myoblast fusion. Two lines of evidence suggest that MR is not required during the first phase of myoblast fusion. First, at early stages of myotube formation in vitro, WT and $MR^{-/-}$ nascent myotubes contained similar numbers of nuclei (Fig. 2). Subsequently, WT myotubes continued to accumulate nuclei through additional rounds of myoblast fusion, whereas $MR^{-/-}$ myotubes did not. Second, early phases of regeneration in vivo were similar in WT and $MR^{-/-}$ muscles, but $MR^{-/-}$ muscles were defective in later stages of muscle regeneration (Fig. 4). Furthermore, the myofibers of adult MR-null mice were significantly reduced in XSA compared with WT myofibers. Importantly, the reduced myofiber XSA of $MR^{-/-}$ mice correlated with a decrease in myonuclear number (Fig. 3). These data indicate that the MR is also required for proper developmental myofiber growth or maintenance in vivo. Thus, MR is necessary for the fusion of myoblasts with nascent myotubes/myofibers both in vitro and in vivo.

Cell mixing experiments demonstrated that MR function is required in myoblasts, as $MR^{-/-}$ myoblasts were deficient in their ability to fuse with nascent myotubes. This defect was due specifically to the loss of MR, as retroviral-mediated MR expression in $MR^{-/-}$ myoblasts restored their ability to fuse with nascent myotubes (Fig. 5). However, MR protein was present in both myoblasts and nascent myotubes at 24 h of differentiation in vitro (Fig. 1). This discrepancy between expression and function may be explained if levels of cell-surface MR protein are regulated differentially in myoblasts and myotubes. Members of the MR family of proteins are constitutively recycled from the plasma membrane, and estimates have been made that only ~10–30% of total MR protein is present on the cell surface at any point in time (East and Isacke, 2002).

What is the cellular mechanism by which MR acts in myoblasts to regulate the second stage of myoblast fusion? We hypothesized that MR may function in myogenic cell–cell adhesion or cell migration. MR has previously been implicated in adhesion of leukocytes to human lymphatic endothelium via interaction with the cell-adhesion molecule L-selectin (Irjala et al., 2003). However, $MR^{-/-}$ myogenic cells were capable of

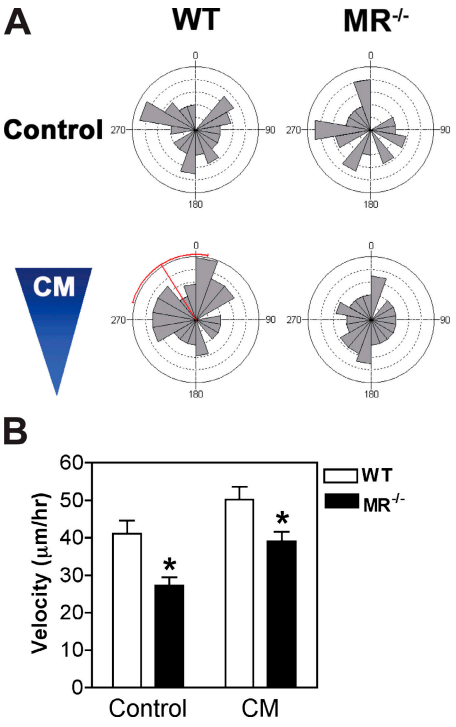

Figure 7. **MR is required for directional migration up a gradient of conditioned media.** WT or $MR^{-/-}$ cells were differentiated for 24 h and assayed for migration in Dunn chemotaxis chambers. Cell migration over 3 h was recorded using time-lapse photography in the presence of control media or a gradient of conditioned media (CM). For each genotype, data were pooled from three independent isolates. (A) Cell directionality was determined using the horizon distance method and the Rayleigh test for unimodal clustering. The circular histograms indicate the proportion of cells with a migratory trajectory lying within each 18° interval. The mean direction and 95% confidence intervals (red line and arc) are shown for conditions in which significant clustering of cell migration occurs. The directionalities of 45 cells were analyzed in each condition, and graphs depict data from 23 cells. (B) The mean velocity of $MR^{-/-}$ cells was 37% lower than WT cells in control media and 29% lower in conditioned media. Data are mean ± SEM. n = 45–50 cells for each condition. *, $P < 0.05$.

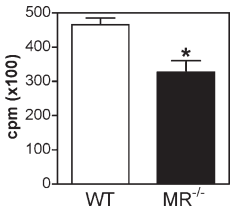

Figure 8. **Collagen uptake is reduced in MR-null muscle cells.** After differentiating for 24 h, WT and $MR^{-/-}$ cells were incubated with 1 nM ^{125}I-labeled type IV collagen in DM for 4 h. Cell surface bound collagen was released by collagenase treatment, and internalized collagen was assessed using a gamma counter and expressed as counts per minute (cpm). Collagen internalization is reduced by 30% in $MR^{-/-}$ cells. Data are mean ± SEM for three independent cell isolates. *, $P < 0.05$.

adhering to one another in suspension-based assays (Knudsen and Horwitz, 1977; Gibralter and Turner, 1985; Knudsen, 1985; Knudsen et al., 1989). In contrast, $MR^{-/-}$ myoblasts displayed decreased velocity and distance of migration during myotube growth (Fig. 6). Importantly, restoration of MR expression via retroviral infection of $MR^{-/-}$ cells significantly increased the velocity of $MR^{-/-}$ cells, indicating that MR is required for efficient myoblast migration. As expected, the migration of $MR^{-/-}$ cells was not disrupted at early times in DM, as MR mRNA levels were very low (Fig. 1) and protein levels were undetectable (not depicted) at the initiation of differentiation. These data are in agreement with the findings that MR is not required for the first phase of fusion. Interestingly, a protein related to MR, Endo180 (also referred to as urokinase-type plasminogen activator receptor–associated protein, or UPARAP) is required for efficient motility of fibroblasts, suggesting that members of the MR family of proteins may share a common role in facilitating cell migration (East et al., 2003; Engelholm et al., 2003). These data provide the first evidence that MR plays a role in cell motility.

Cell migration during tissue development and remodeling involves both a directed cellular response to chemoattractant factors and the breakdown of the ECM (Murphy and Gavrilovic, 1999; Ridley et al., 2003). Degradation of the ECM by extracellular proteolytic enzymes facilitates cell motility, whereas chemotaxis involves the movement of cells to a specific location in response to directional signals. Our data reveal that MR is required for the directed migration of muscle cells up a conditioned media gradient (Fig. 7). We propose that nascent myotubes secrete factors necessary for the directed migration of myoblasts during fusion and that MR is required for the directional response of cells to at least one of these factors. The factors responsible for MR-dependent chemotaxis are unknown. A chemoattractant may bind the extracellular region of MR directly. Engagement of the MR by an extracellular ligand may initiate an intracellular signaling cascade necessary for providing directional cues to the cell. However, no characterized signaling domains have been identified in the MR cytoplasmic tail. Alternatively, MR may act as a coreceptor for a chemoattractant. For example, Endo180 interaction with the GPI-anchored urokinase plasminogen activator receptor is required for directed cell migration up a urokinase plasminogen activator gradient (Sturge et al., 2003). The mechanism by which MR mediates directed muscle cell migration is currently under investigation.

In addition to impaired directional migration, $MR^{-/-}$ cells migrated at a reduced velocity during myoblast fusion (Fig. 6) and in the presence of control or conditioned media (Fig. 7). These data suggest that MR may also facilitate the random motility of muscle cells. Endo180 is thought to facilitate the motility of fibroblasts via clearance of the ECM component collagen (East et al., 2003). MR has recently been shown to bind several forms of collagen, and internalization of collagen IV by macrophages is dependent on the presence of MR (Martinez-Pomares et al., 2006; Napper et al., 2006). Our results revealed that $MR^{-/-}$ muscle cells were impaired in the uptake of type IV collagen (Fig. 8). However, unlike $MR^{-/-}$ macrophages, collagen uptake was not ablated in $MR^{-/-}$ muscle cells. Endo180, which is expressed in fusing muscle cells (unpublished data), may enable the uptake of collagen in the absence of MR. We hypothesize that MR regulates cell motility by facilitating collagen clearance by muscle cells.

Although $MR^{-/-}$ cells migrated at a reduced velocity, their migration was not ablated, suggesting that additional migratory signals are functioning in the absence of MR. The migration of muscle precursor cells during embryonic development and postnatal regeneration is essential to the formation and maintenance of mammalian skeletal muscle. A variety of molecules, including growth factors, cytokines, chemokines, ECM components, proteolytic enzymes, and intracellular signaling proteins have been implicated in cell migration. Hepatocyte growth factor (HGF) and its receptor, c-Met, are required for the migration of muscle precursor cells from the dermomyotome to the limbs (Birchmeier and Brohmann, 2000). Several growth factors, including HGF, bFGF, PDGF A and B, LIF (leukemia inhibitory factor), TGF-β, and IGF-1 (insulin-like growth factor I) induce myoblast migration in vitro (Robertson et al., 1993; Bischoff, 1997; Suzuki et al., 2000). The cytokines TNF-α and IFN-γ and the chemokine RANTES also enhance myoblast migration in vitro (Bischoff, 1997; Corti et al., 2001). ECM components such as laminin (Goodman et al., 1989) and proteoglycans (Olguin et al., 2003) as well as extracellular proteolytic enzymes, including matrix metalloproteinases and calpain (El Fahime et al., 2000; Dedieu et al., 2004), influence myoblast motility. Studies of intracellular signaling pathways involved in myoblast migration indicate that HGF induces myoblast migration via activation of Ras and phosphatidylinositol 3-kinase and their downstream effectors (Suzuki et al., 2000; Kawamura et al., 2004). The precise relationship among these various molecules during myoblast migration remains unclear.

Our results suggest, but do not directly prove, the importance of myoblast migration for myotube growth. Further roles for MR may contribute to the defect in the fusion of $MR^{-/-}$ myoblasts with nascent myotubes. For example, MR may regulate cell–cell interactions among myogenic cells. MR is known to bind a variety of glycosylated proteins in other cell types and may aid in the recognition of myoblasts and myotubes by interacting with a ligand or ligands on the surface of opposing cells. Identification of MR ligands in skeletal muscle will provide further insight into the mechanisms by which muscle growth is regulated. Understanding the molecular pathways involved in myoblast migration, adhesion, and fusion is important in designing treatments for impaired muscle growth associated with age, disease, and atrophy. In addition, promotion of cell fusion may aid in cell therapy protocols using exogenous stem cells (Seale et al., 2001; Smythe et al., 2001).

Materials and methods

Animals

$MR^{-/-}$ mice produced on the 129vJ × C57BL/6 background and backcrossed to C57BL/6 mice for seven generations were provided by M. Nussenzweig (The Rockefeller University, New York, NY; Lee et al., 2002). Additional $MR^{-/-}$ mice were generated by homozygous matings. Control age- and sex-matched C57BL/6 mice were purchased from Charles River Laboratories. Adult mice between 8–12 wk of age were used for all studies. All animals were handled in accordance with the institutional guidelines of Emory University.

Primary muscle cell culture and cytokine treatment

Primary myoblasts were derived from the hindlimb muscles of adult female WT or $MR^{-/-}$ mice as previously described with the exception of a percoll gradient (Mitchell and Pavlath, 2001; Bondesen et al., 2004). In brief, muscles were minced mechanically and digested with 0.1% pronase (Calbiochem) in DME containing 25 mM Hepes at 37°C with slight agitation for 1 h. The muscles were further dissociated by trituration and passed through a 100-μm filter. Cells were suspended in growth media (GM; Ham's F10, 20% FBS, 5 ng/ml bFGF, 100 U/ml penicillin G, and 100 μg/ml streptomycin) and grown on collagen-coated dishes in a humidified 5% CO_2 incubator at 37°C. Primary cultures were enriched for myogenic cells to >99% purity using the preplating technique as described previously (Rando and Blau, 1994). To induce differentiation, cells were plated on dishes coated with entactin–collagen IV–laminin (E-C-L; Upstate Biotechnology) in GM and shortly thereafter switched to DM (DME, 1% Insulin-Transferrin-Selenium-A supplement [Invitrogen], 100 U/ml penicillin G, and 100 μg/ml streptomycin). For analysis of MR mRNA expression, WT and IL-4Rα$^{-/-}$ were derived and grown as described previously (Horsley et al., 2003). In experiments using exogenous cytokines, vehicle or 10 ng/ml recombinant mouse IL-4 (R&D Systems) was added to cells after 24 h in DM and RNA was isolated 24 h later.

RT-PCR analyses

RNA was isolated from primary muscle cells using TRIzol reagent (Life Technologies) according to the manufacturer's instructions. Reverse-transcriptase reactions were performed using 2.5 μg of total RNA. cDNA was amplified using Expand High Fidelity PCR system (Roche) with primers specific for MR (available under GenBank/EMBL/DDBJ under accession no. NM_008625; sense, 5′ AGTGATGGTTCTCCCGTTTCCTAT; antisense, 5′ TGACTGCCCACCATTCTTGTTTAT) or myogenin (accession no. NM_031189; sense, 5′ AGCGGCTGCCTAAAGTGGAGAT; antisense, 5′ GGACGTAAGGGAGTGCAGATTGTG). All primer pairs spanned intron and exon boundaries to control for any contaminating DNA in RNA samples. MR cDNA was amplified by incubation at 94°C for 5 min, followed by 35 cycles of 94°C for 30 s, 54°C for 30 s, and 72°C for 30 s, and terminating at 72°C for 5 min, generating a 390-bp amplicon. Myogenin cDNA was amplified by incubation at 94°C for 5 min, followed by 25 cycles of 94°C for 30 s, 60°C for 30 s, and 72°C for 30 s, and terminating with 72°C for 5 min, generating a 266-bp amplicon. Amplicons were separated by electrophoresis in a 1% agarose gel and visualized with ethidium bromide. RT-PCR analysis of 18S ribosomal RNA was included as a control for each sample using QuantumRNA 18S primers (Ambion).

MR immunocytochemistry

For detection of MR protein by immunofluorescence, WT and $MR^{-/-}$ primary myoblasts were differentiated for 24 h and subsequently fixed in 3.7% formaldehyde for 10 min. Cells were then incubated in block buffer (PBS containing 0.25% Triton X-100 and 5% donkey serum) for 1 h, followed by incubation with a polyclonal antibody recognizing the cytoplasmic tail of MR (provided by A. Regnier-Vigouroux, Deutsches Krebsforschungszentrum, Heidelberg, Germany; Burudi and Regnier-Vigouroux, 2001) diluted 1:500 in block buffer for 1 h. After several washes in PBS + 0.2% Tween 20 (PBS-T), the cells were incubated with biotin-conjugated donkey anti–rabbit IgG (Jackson ImmunoResearch Laboratories) diluted 1:500 in block buffer for 1 h. Cells were washed with PBS-T and subsequently incubated with streptavidin-horseradish peroxidase diluted 1:250 in block buffer for 30 min. The Tyramide Signal Amplification green reagent (NEN Life Science Products) was used to visualize antibody binding. Fluorescence images were acquired using a microscope (Axiovert 200M; Carl Zeiss MicroImaging, Inc.) with a 0.3 NA 10× Plan-Neofluar objective (Carl Zeiss MicroImaging, Inc.) and camera (QImaging) with OpenLab 3.1.4 (Improvision). Cells were stored in PBS at room temperature for all image acquisition. Images were assembled using Photoshop 7.0 (Adobe) software and were not modified with the exception of equal adjustments in size, brightness, and contrast.

Differentiation and fusion assays

Primary myoblasts from WT and $MR^{-/-}$ mice were seeded on E-C-L–coated 6-well dishes at a density of 2×10^5 cells/well in GM. Cells were allowed to adhere to the dish for ~1 h before switching to DM. After 20 or 48 h in DM, cells were fixed in 3.7% formaldehyde for 10 min and subsequently immunostained with an antibody against eMyHC (F1.652; Developmental Studies Hybridoma Bank) as described previously (Horsley et al., 2001). The differentiation index was determined by dividing the total number of nuclei in eMyHC-positive cells by the total number of nuclei counted. The mean number of nuclei per myotube was determined by dividing the total number of nuclei in myotubes (≥2 nuclei) by the total number of myotubes counted. The fusion index was determined by dividing the total number of nuclei in myotubes by the total number of nuclei counted. At least 100 myotubes and 500 nuclei per condition were analyzed for each assay.

To assess myogenin expression, three independent WT and $MR^{-/-}$ cell isolates were differentiated for 0 or 16 h and were subsequently lysed in RIPA-2 buffer (50 mM Tris-HCl, pH 8.0, 150 mM NaCl, 1% NP-40, 0.5% deoxycholic acid, and 0.1% SDS) containing protease inhibitors (Mini complete; Roche) for 10 min on ice. Lysates were spun at 21,000 *g* for 15 min at 4°C. Protein concentration was determined using the Bradford assay (Bio-Rad Laboratories), and 25 μg of total protein was separated by SDS-PAGE. After transfer to a polyvinylidene difluoride membrane (Millipore), myogenin protein was detected using a mouse monoclonal antibody (F5D; Developmental Studies Hybridoma Bank) diluted 1:10 in block buffer as described previously (Friday and Pavlath, 2001). Membranes were stained with Coomassie (Bio-Rad Laboratories) to confirm equal loading.

Collection of muscles and morphometric measurements

TA and soleus muscles were collected from adult male mice ($n = 5$–6) as described previously (Horsley et al., 2001). Serial 14-μm sections were collected along the entire length of each muscle and stained with H&E. Histological analyses were performed on sections collected from similar regions of each TA muscle and the belly of each soleus muscle. Two images were captured from each section, and Scion Image 1.63 (Scion Corp.) was used to determine the XSA of 50–100 myofibers per field. All photography was performed on a microscope (Axioplan; Carl Zeiss MicroImaging, Inc.) with a 0.3 NA 10× Plan-Neofluar objective (Carl Zeiss MicroImaging, Inc.) equipped with a charge-coupled device camera (Carl Zeiss MicroImaging, Inc.). Pictures were assembled using Photoshop 7.0 and were not modified other than adjustments of size, color levels, brightness, and contrast.

In vivo myonuclear number analyses were performed as described previously (Horsley et al., 2001). In brief, sections of TA muscles from WT and $MR^{-/-}$ mice ($n = 5$–6) were immunostained with an antibody against dystrophin (MANDYS8; Sigma-Aldrich) to visualize the sarcolemma of myofibers and mounted in Vectashield mounting media containing DAPI (Vector Laboratories) to stain nuclei. Nuclei within dystrophin-positive sarcolemma were counted for 50–100 myofibers, and the number of nuclei was expressed per 100 myofibers.

To analyze muscle growth during regeneration, injury was induced in the TA muscles of WT and $MR^{-/-}$ mice ($n = 5$–6) by injection of 50 μl of 1.2% $BaCl_2$ diluted in PBS with a 27-gauge needle (Caldwell et al., 1990; McArdle et al., 1994) along the length of the muscle. Muscles were collected 5, 7, or 14 d after injury, and XSA of centrally nucleated regenerating fibers was assessed as described above.

Retroviral plasmids, production, and infection

A retroviral vector encoding full-length MR (provided by L. Martinez-Pomares, Queen's Medical Center, Nottingham, UK; Martinez-Pomares et al., 2003) and a control vector (pFB-neo; Stratagene) were used to produce infectious retroviral supernatants as described previously (Abbott et al., 1998). Primary WT and $MR^{-/-}$ myoblasts were subjected to two rounds of infection (Abbott et al., 1998), and infected cells were selected by growing cells with 50 μg/ml of Geneticin (Invitrogen) in GM.

Cell mixing experiments

Cell mixing experiments were performed as described previously with minor modifications (Horsley et al., 2003). Primary myoblasts were grown at low density (0.5×10^5 cells per well of a 6-well plate) or high density (2×10^5 cells per well of a 6-well plate) in DM for 24 h to generate differentiated mononucleated cells or nascent myotubes, respectively. Mononucleated cells were incubated with CellTracker Orange CMTMR (5-(and-6)-(((4-chloromethyl) benzoyl) amino) tetramethylrhodamine) (Invitrogen) diluted to 2.5 μM in DM, and nascent myotubes were incubated with CellTracker Green CMFDA (5-chloromethyl-7-hydroxycoumarin; Invitrogen) diluted to 0.5 μM in DM for 10 min at 37°C. Cells were washed twice with PBS, trypsinized, mixed at equal cell number, and plated to give a final cell number of 2×10^5 cells per well of a 6-well E-C-L–coated plate. After 24 h in DM, the cells were fixed for 10 min in 3.7% formaldehyde. The presence of dual label was analyzed in 50–100 myotubes with ≥3 nuclei. Mixing experiments were performed in triplicate using WT and $MR^{-/-}$ myoblasts from three independent cell isolates.

Cell migration assays

Primary myoblasts were seeded on E-C-L–coated 35-mm plates at a density of 2×10^5 cells per plate in GM. After allowing cells to adhere for ~1 h, cells were switched to DM. At 0 or 24 h in DM, 25 mM Hepes was added to the cultures and cells were transferred to a microscope stage heated to 37°C. Cell migration was visualized using a Axiovert 200M microscope with a 0.3 NA 10× Plan-Neofluar objective (Carl Zeiss MicroImaging, Inc.), and images were recorded (QImaging camera and OpenLab 3.1.4 software) every 5 min for 3 h. Cell velocities were calculated in micrometers per hour using ImageJ software by tracking the paths of individual mononucleated cells. Cell migration assays were performed for each genotype using three independent cell isolates. The mean velocities of 45–50 cells (~15 cells per isolate) were pooled and analyzed for statistical significance as described (see Statistics).

Dunn chamber analysis

Permanox plastic cell culture slides (Nunc) were cut into 6-cm^2 squares, and an ~1-cm^2 region of each slide was coated with E-C-L for 1 h at 37°C. Primary myoblasts were then seeded at a density of 5×10^3 cells per slide in GM. Cells were allowed to adhere for 1 h, and GM was replaced with DM. The low density at which the cells were plated ensured that cells underwent myogenic differentiation with limited cell fusion. After 24 h in DM, the Dunn chamber was assembled as described previously (Zicha et al., 1991, 1997). DM that had been conditioned by differentiating primary muscle cells for 24 h was collected before chamber assembly and supplemented with 25 mM Hepes. To set up gradient experiments, both concentric wells of the chemotaxis chamber were filled with control DM (supplemented with 25 mM Hepes), and the slide containing differentiating cells was inverted onto the chamber to cover both wells. The slide was sealed onto the chamber with a hot 1:1:1 mixture of paraffin wax, beeswax, and petroleum jelly, leaving a small slit of the outer well open. DM was removed from the outer well and replaced with control or conditioned media, and the slit was sealed. After allowing the gradient to establish for 30 min at 37°C, a small region over the annular bridge was visualized and cell migration was analyzed by time-lapse microscopy as above (see Cell migration assays). Statistical analyses of directional data were performed to assess the chemotactic response of the cells as described previously (Zicha et al., 1997). Each cell path was converted to a trajectory originating from (0,0) on an x-y axis. A horizon distance for each condition was established by determining the distance passed by 50% of the cells in a straight line from their starting point. The horizon method is designed to assess the directionality of cell movement without influence from differences in cell motility. Cells that fail to reach the horizon distance were excluded from directional analysis. A trajectory angle for each cell was calculated as the direction of each cell from its starting point to the point at which the cell crossed the horizon distance. The directional data were summarized as circular histograms in which the area of each sector represents the proportion of trajectory angles located within each 18° interval. The Rayleigh test for unimodal clustering was applied with $P < 0.05$ as the criterion for rejecting the null hypothesis of uniform distribution. Where unimodal clustering was observed, a mean direction and 95% confidence interval were calculated. Statistical analysis was performed using Oriana 2.0 (RockWare). Dunn chamber assays were performed using three independent cell isolates. Directional analyses were performed using at least 15 cells per assay for a total of 45 cells.

Collagen uptake assay

Collagen internalization assays were performed as described previously (Engelholm et al., 2003). Type IV collagen (Calbiochem) was labeled with ^{125}I via Iodogen (PerkinElmer), resulting in a specific activity of 88 μCi/mg. Primary myoblasts were differentiated for 24 h as described above (see Differentiation and fusion assays). After 24 h in DM, 1 nM ^{125}I-collagen was added to the cells. After a 4-h incubation at 37°C, the medium was removed and cells were washed twice with PBS to remove unbound collagen. Cells were treated with 0.2% type I collagenase (Worthington) diluted in 0.05% trypsin and 0.53 mM EDTA (Invitrogen) to lift cells and cleave cell surface bound collagen. In pilot experiments, 0.2% type I collagenase treatment released >95% of cell surface bound collagen. The detached cells were centrifuged at 1,000 *g* for 5 min, and the radioactivity of the supernatant (cell surface released collagen) and pellet (internalized collagen) was measured using a gamma counter (1470 WIZARD; Wallac).

Statistics

To determine significance between two groups, comparisons were made using *t* tests. Analyses of multiple groups were performed using a two-way analysis of variance with Bonferroni's posttest. Statistical analyses were performed using GraphPad Prism 4.0 (GraphPad) for Macintosh or SigmaStat 2.03 (SPSS). For all statistical tests, a confidence level of $P < 0.05$ was accepted for statistical significance.

Online supplemental material
Fig. S1 shows that cell proliferation and cell survival are not disrupted in $MR^{-/-}$ cells. Fig. S2 demonstrates that retroviral infection does not alter myoblast motility. Online supplemental material is available at http://www.jcb.org/cgi/content/full/jcb.200601102/DC1.

We thank Stephen T. Mills for assistance with in vivo analyses, Dr. Michel Nussenzweig for the $MR^{-/-}$ mice, Dr. Louisa Martinez-Pomares for the MR retroviral construct, and Dr. Anne Regnier-Vigouroux for the MR antibody.

This work was supported by grants AR-047315, AR-48884, AR-051372, and AR-052730 from the National Institutes of Health and the Muscular Dystrophy Association to G.K. Pavlath. K.M. Jansen was supported by National Institutes of Health training grant T32-GM08367.

Submitted: 19 January 2006
Accepted: 22 June 2006

References

Abbott, K.L., B.B. Friday, D. Thaloor, T.J. Murphy, and G.K. Pavlath. 1998. Activation and cellular localization of the cyclosporine A-sensitive transcription factor NF-AT in skeletal muscle cells. *Mol. Biol. Cell.* 9:2905–2916.

Allen, D.L., R.R. Roy, and V.R. Edgerton. 1999. Myonuclear domains in muscle adaptation and disease. *Muscle Nerve.* 22:1350–1360.

Birchmeier, C., and H. Brohmann. 2000. Genes that control the development of migrating muscle precursor cells. *Curr. Opin. Cell Biol.* 12:725–730.

Bischoff, R. 1997. Chemotaxis of skeletal muscle satellite cells. *Dev. Dyn.* 208:505–515.

Bondesen, B.A., S.T. Mills, K.M. Kegley, and G.K. Pavlath. 2004. The COX-2 pathway is essential during early stages of skeletal muscle regeneration. *Am. J. Physiol. Cell Physiol.* 287:C475–C483.

Burudi, E.M., and A. Regnier-Vigouroux. 2001. Regional and cellular expression of the mannose receptor in the post-natal developing mouse brain. *Cell Tissue Res.* 303:307–317.

Caldwell, C.J., D.L. Mattey, and R.O. Weller. 1990. Role of the basement membrane in the regeneration of skeletal muscle. *Neuropathol. Appl. Neurobiol.* 16:225–238.

Corti, S., S. Salani, R. Del Bo, M. Sironi, S. Strazzer, M.G. D'Angelo, G.P. Comi, N. Bresolin, and G. Scarlato. 2001. Chemotactic factors enhance myogenic cell migration across an endothelial monolayer. *Exp. Cell Res.* 268:36–44.

Dedieu, S., S. Poussard, G. Mazeres, F. Grise, E. Dargelos, P. Cottin, and J.J. Brustis. 2004. Myoblast migration is regulated by calpain through its involvement in cell attachment and cytoskeletal organization. *Exp. Cell Res.* 292:187–200.

Doherty, K.R., A. Cave, D.B. Davis, A.J. Delmonte, A. Posey, J.U. Earley, M. Hadhazy, and E.M. McNally. 2005. Normal myoblast fusion requires myoferlin. *Development.* 132:5565–5575.

East, L., and C.M. Isacke. 2002. The mannose receptor family. *Biochim. Biophys. Acta.* 1572:364–386.

East, L., A. McCarthy, D. Wienke, J. Sturge, A. Ashworth, and C.M. Isacke. 2003. A targeted deletion in the endocytic receptor gene Endo180 results in a defect in collagen uptake. *EMBO Rep.* 4:710–716.

El Fahime, E., Y. Torrente, N.J. Caron, M.D. Bresolin, and J.P. Tremblay. 2000. In vivo migration of transplanted myoblasts requires matrix metalloproteinase activity. *Exp. Cell Res.* 258:279–287.

Engelholm, L.H., K. List, S. Netzel-Arnett, E. Cukierman, D.J. Mitola, H. Aaronson, L. Kjoller, J.K. Larsen, K.M. Yamada, D.K. Strickland, et al. 2003. uPARAP/Endo180 is essential for cellular uptake of collagen and promotes fibroblast collagen adhesion. *J. Cell Biol.* 160:1009–1015.

Ezekowitz, R.A., D.J. Williams, H. Koziel, M.Y. Armstrong, A. Warner, F.F. Richards, and R.M. Rose. 1991. Uptake of *Pneumocystis carinii* mediated by the macrophage mannose receptor. *Nature.* 351:155–158.

Fiete, D.J., M.C. Beranek, and J.U. Baenziger. 1998. A cysteine-rich domain of the "mannose" receptor mediates GalNAc-4-SO4 binding. *Proc. Natl. Acad. Sci. USA.* 95:2089–2093.

Friday, B.B., and G.K. Pavlath. 2001. A calcineurin- and NFAT-dependent pathway regulates Myf5 gene expression in skeletal muscle reserve cells. *J. Cell Sci.* 114:303–310.

Gibralter, D., and D.C. Turner. 1985. Dual adhesion systems of chick myoblasts. *Dev. Biol.* 112:292–307.

Goodman, S.L., G. Risse, and K. von der Mark. 1989. The E8 subfragment of laminin promotes locomotion of myoblasts over extracellular matrix. *J. Cell Biol.* 109:799–809.

Horsley, V., and G.K. Pavlath. 2003. Prostaglandin $F_{2\alpha}$ stimulates growth of skeletal muscle cells via an NFATC2-dependent pathway. *J. Cell Biol.* 161:111–118.

Horsley, V., and G.K. Pavlath. 2004. Forming a multinucleated cell: molecules that regulate myoblast fusion. *Cells Tissues Organs.* 176:67–78.

Horsley, V., B.B. Friday, S. Matteson, K.M. Kegley, J. Gephart, and G.K. Pavlath. 2001. Regulation of the growth of multinucleated muscle cells by an NFATC2-dependent pathway. *J. Cell Biol.* 153:329–338.

Horsley, V., K.M. Jansen, S.T. Mills, and G.K. Pavlath. 2003. IL-4 acts as a myoblast recruitment factor during mammalian muscle growth. *Cell.* 113:483–494.

Iezzi, S., M. Di Padova, C. Serra, G. Caretti, C. Simone, E. Maklan, G. Minetti, P. Zhao, E.P. Hoffman, P.L. Puri, and V. Sartorelli. 2004. Deacetylase inhibitors increase muscle cell size by promoting myoblast recruitment and fusion through induction of follistatin. *Dev. Cell.* 6:673–684.

Irjala, H., K. Alanen, R. Grenman, P. Heikkila, H. Joensuu, and S. Jalkanen. 2003. Mannose receptor (MR) and common lymphatic endothelial and vascular endothelial receptor (CLEVER)-1 direct the binding of cancer cells to the lymph vessel endothelium. *Cancer Res.* 63:4671–4676.

Kawamura, K., K. Takano, S. Suetsugu, S. Kurisu, D. Yamazaki, H. Miki, T. Takenawa, and T. Endo. 2004. N-WASP and WAVE2 acting downstream of phosphatidylinositol 3-kinase are required for myogenic cell migration induced by hepatocyte growth factor. *J. Biol. Chem.* 279:54862–54871.

Knudsen, K.A. 1985. The calcium-dependent myoblast adhesion that precedes cell fusion is mediated by glycoproteins. *J. Cell Biol.* 101:891–897.

Knudsen, K.A., and A.F. Horwitz. 1977. Tandem events in myoblast fusion. *Dev. Biol.* 58:328–338.

Knudsen, K.A., L. Smith, and S. McElwee. 1989. Involvement of cell surface phosphatidylinositol-anchored glycoproteins in cell-cell adhesion of chick embryo myoblasts. *J. Cell Biol.* 109:1779–1786.

Kruskal, B.A., K. Sastry, A.B. Warner, C.E. Mathieu, and R.A. Ezekowitz. 1992. Phagocytic chimeric receptors require both transmembrane and cytoplasmic domains from the mannose receptor. *J. Exp. Med.* 176:1673–1680.

Kurachi, T., I. Morita, T. Oki, T. Ueki, K. Sakaguchi, S. Enomoto, and S. Murota. 1994. Expression on outer membranes of mannose residues, which are involved in osteoclast formation via cellular fusion events. *J. Biol. Chem.* 269:17572–17576.

Lee, S.J., S. Evers, D. Roeder, A.F. Parlow, J. Risteli, L. Risteli, Y.C. Lee, T. Feizi, H. Langen, and M.C. Nussenzweig. 2002. Mannose receptor-mediated regulation of serum glycoprotein homeostasis. *Science.* 295:1898–1901.

Linehan, S.A., L. Martinez-Pomares, R.P. da Silva, and S. Gordon. 2001. Endogenous ligands of carbohydrate recognition domains of the mannose receptor in murine macrophages, endothelial cells and secretory cells; potential relevance to inflammation and immunity. *Eur. J. Immunol.* 31:1857–1866.

Linehan, S.A., P.S. Coulson, R.A. Wilson, A.P. Mountford, F. Brombacher, L. Martinez-Pomares, and S. Gordon. 2003. IL-4 receptor signaling is required for mannose receptor expression by macrophages recruited to granulomata but not resident cells in mice infected with *Schistosoma mansoni*. *Lab. Invest.* 83:1223–1231.

Martinez-Pomares, L., and S. Gordon. 1999. Potential role of the mannose receptor in antigen transport. *Immunol. Lett.* 65:9–13.

Martinez-Pomares, L., S.A. Linehan, P.R. Taylor, and S. Gordon. 2001. Binding properties of the mannose receptor. *Immunobiology.* 204:527–535.

Martinez-Pomares, L., D.M. Reid, G.D. Brown, P.R. Taylor, R.J. Stillion, S.A. Linehan, S. Zamze, S. Gordon, and S.Y. Wong. 2003. Analysis of mannose receptor regulation by IL-4, IL-10, and proteolytic processing using novel monoclonal antibodies. *J. Leukoc. Biol.* 73:604–613.

Martinez-Pomares, L., D. Wienke, R. Stillion, E.J. McKenzie, J.N. Arnold, J. Harris, E. McGreal, R.B. Sim, C.M. Isacke, and S. Gordon. 2006. Carbohydrate-independent recognition of collagens by the macrophage mannose receptor. *Eur. J. Immunol.* 36:1074–1082.

McArdle, A., R.H. Edwards, and M.J. Jackson. 1994. Release of creatine kinase and prostaglandin E2 from regenerating skeletal muscle fibers. *J. Appl. Physiol.* 76:1274–1278.

McNally, A.K., K.M. DeFife, and J.M. Anderson. 1996. Interleukin-4-induced macrophage fusion is prevented by inhibitors of mannose receptor activity. *Am. J. Pathol.* 149:975–985.

Mitchell, P.O., and G.K. Pavlath. 2001. A muscle precursor cell-dependent pathway contributes to muscle growth after atrophy. *Am. J. Physiol. Cell Physiol.* 281:C1706–C1715.

Morishima, S., I. Morita, T. Tokushima, H. Kawashima, M. Miyasaka, K. Omura, and S. Murota. 2003. Expression and role of mannose receptor/terminal high-mannose type oligosaccharide on osteoclast precursors during osteoclast formation. *J. Endocrinol.* 176:285–292.

Muroya, S., H. Takagi, S. Tajima, and A. Asano. 1994. Selective inhibition of a step of myotube formation with wheat germ agglutinin in a murine myoblast cell line, C2C12. *Cell Struct. Funct.* 19:241–252.

Murphy, G., and J. Gavrilovic. 1999. Proteolysis and cell migration: creating a path? *Curr. Opin. Cell Biol.* 11:614–621.

Napper, C.E., K. Drickamer, and M.E. Taylor. 2006. Collagen binding by the mannose receptor mediated through the fibronectin type II domain. *Biochem. J.* 395:579–586.

Olguin, H.C., C. Santander, and E. Brandan. 2003. Inhibition of myoblast migration via decorin expression is critical for normal skeletal muscle differentiation. *Dev. Biol.* 259:209–224.

Otter, M., M.M. Barrett-Bergshoeff, and D.C. Rijken. 1991. Binding of tissue-type plasminogen activator by the mannose receptor. *J. Biol. Chem.* 266:13931–13935.

Park, I.H., and J. Chen. 2005. Mammalian target of rapamycin (mTOR) signaling is required for a late-stage fusion process during skeletal myotube maturation. *J. Biol. Chem.* 280:32009–32017.

Pontow, S.E., V. Kery, and P.D. Stahl. 1992. Mannose receptor. *Int. Rev. Cytol.* 137B:221–244.

Rando, T.A., and H.M. Blau. 1994. Primary mouse myoblast purification, characterization, and transplantation for cell-mediated gene therapy. *J. Cell Biol.* 125:1275–1287.

Ridley, A.J., M.A. Schwartz, K. Burridge, R.A. Firtel, M.H. Ginsberg, G. Borisy, J.T. Parsons, and A.R. Horwitz. 2003. Cell migration: integrating signals from front to back. *Science.* 302:1704–1709.

Robertson, T.A., M.A. Maley, M.D. Grounds, and J.M. Papadimitriou. 1993. The role of macrophages in skeletal muscle regeneration with particular reference to chemotaxis. *Exp. Cell Res.* 207:321–331.

Sallusto, F., M. Cella, C. Danieli, and A. Lanzavecchia. 1995. Dendritic cells use macropinocytosis and the mannose receptor to concentrate macromolecules in the major histocompatibility complex class II compartment: downregulation by cytokines and bacterial products. *J. Exp. Med.* 182:389–400.

Schlesinger, L.S. 1993. Macrophage phagocytosis of virulent but not attenuated strains of *Mycobacterium tuberculosis* is mediated by mannose receptors in addition to complement receptors. *J. Immunol.* 150:2920–2930.

Seale, P., A. Asakura, and M.A. Rudnicki. 2001. The potential of muscle stem cells. *Dev. Cell.* 1:333–342.

Smythe, G.M., S.I. Hodgetts, and M.D. Grounds. 2001. Problems and solutions in myoblast transfer therapy. *J. Cell. Mol. Med.* 5:33–47.

Stein, M., S. Keshav, N. Harris, and S. Gordon. 1992. Interleukin 4 potently enhances murine macrophage mannose receptor activity: a marker of alternative immunologic macrophage activation. *J. Exp. Med.* 176:287–292.

Sturge, J., D. Wienke, L. East, G.E. Jones, and C.M. Isacke. 2003. GPI-anchored uPAR requires Endo180 for rapid directional sensing during chemotaxis. *J. Cell Biol.* 162:789–794.

Suzuki, J., Y. Yamazaki, G. Li, Y. Kaziro, and H. Koide. 2000. Involvement of Ras and Ral in chemotactic migration of skeletal myoblasts. *Mol. Cell. Biol.* 20:4658–4665.

Taylor, M.E., K. Bezouska, and K. Drickamer. 1992. Contribution to ligand binding by multiple carbohydrate-recognition domains in the macrophage mannose receptor. *J. Biol. Chem.* 267:1719–1726.

Wright, W.E., D.A. Sassoon, and V.K. Lin. 1989. Myogenin, a factor regulating myogenesis, has a domain homologous to MyoD. *Cell.* 56:607–617.

Zicha, D., G. Dunn, and A.F. Brown. 1991. A new direct-viewing chemotaxis chamber. *J. Cell Sci.* 99:769–775.

Zicha, D., G. Dunn, and G. Jones. 1997. Analyzing chemotaxis using the Dunn direct-viewing chamber. *Methods Mol. Biol.* 75:449–457.

Zimmer, H., S. Riese, and A. Regnier-Vigouroux. 2003. Functional characterization of mannose receptor expressed by immunocompetent mouse microglia. *Glia.* 42:89–100.